Title page

Role of DCP1-DCP2 complex regulated by viral and host microRNAs in DNA virus infection

Yuechao Sun, Xiaobo Zhang*

College of Life Sciences and Laboratory for Marine Biology and Biotechnology of Qingdao National Laboratory for Marine Science and Technology, Zhejiang University, Hangzhou 310058, People's Republic of China

* Corresponding author: Prof Xiaobo Zhang

Tel: 86-571-88981129

Fax: 86-571-88981151

Email: zxb0812@zju.edu.cn

Abstract

The DCP1-DCP2 complex can regulate the animal antiviral immunity by the decapping of retrovirus RNAs and the suppression of RNAi pathway. However, the influence of DCP1-DCP2 complex on DNA virus infection and the regulation of DCP1-DCP2 complex by microRNAs (miRNAs) remain unclear. In this study, we investigated the role of miRNA-regulated DCP1-DCP2 complex in DNA virus infection. Our results suggested that the DCP1-DCP2 complex played a positive role in the infection of white spot syndrome virus (WSSV), a DNA virus of shrimp. The N-terminal regulatory domain of DCP2 was interacted with the EVH1 domain of DCP1, forming the DCP1-DCP2 complex. Furthermore, a host shrimp miRNA (miR-87) inhibited WSSV infection by targeting the host DCP2 gene and a viral miRNA (WSSV-miR-N46) took a negative effect on WSSV replication by targeting the host DCP1 gene. Therefore, our study provided novel insights into the underlying mechanism of DCP1-DCP2 complex and its regulation by miRNAs in virus-host interactions.

The DCP1-DCP2 complex can regulate the animal antiviral immunity by the decapping of retrovirus RNAs and the suppression of RNAi pathway. In the present study, the findings indicated that the silencing of the DCP1-DCP2 complex inhibited the infection of WSSV, a DNA virus of shrimp, suggesting that the DCP1-DCP2 complex facilitated DNA virus infection. Due to the suppressive role of the DCP1-DCP2 complex in RNAi pathway against virus infection, the DCP1-DCP2 complex could promote WSSV infection in shrimp. In this context, our study contributed a novel aspect of the DCP1-DCP2 complex in virus-host interactions. Our study revealed that the host and viral miRNAs could regulate the DCP1-DCP2 complex to affect virus infection. Therefore, our study provided novel insights into

48 the miRNA-mediated regulation of DCP1-DCP2 complex took great effects on RNAi
49 immunity of invertebrates against virus infection.
50 Key words: DCP1-DCP2 complex; miRNA; DNA virus infection
51
52
53
54
55
56
57
58
59

60 **Introduction**

61 Classical virus infection in the host cell is initiated by interactions between viral
62 capsid or envelope proteins and host cell surface receptors. The internalization of
63 virions is either through the fusion of the viral envelope and the host plasma
64 membrane, or through the endocytosis pathway, causing the virions to escape from
65 the endocytosa or other small vesicles and enter the cytoplasm (1). Cell receptors
66 attached to the host can directly trigger conformational changes in the surface
67 structure of the virus or activate specific signaling pathways that facilitate the entry of
68 the virus (1). The life cycle of a virus begins with the entry of the host cell.Replication
69 of viral genomes, synthesis of viral proteins, assembly of viral particles, and release of
70 viruses from host cells depend largely on host mechanisms (1, 2). It is reported that
71 the stability of viral mrna is regulated by the dcp1-dcp2 complex located in the
72 P-body (the processing bodies) (3, 4). The DCP1-DCP2 complex can trigger mRNA

73 decapping. DCP2 catalyzed dissection releases m7G and a single 5 'phosphorylated
74 mRNA.This is considered to be an irreversible process, and the target is that mRNA is
75 degraded by exonuclease Xrn1, 5 'to 3' (5). DCP2 protein contains n-terminal
76 Nudix/MutT motifs, which are usually present in pyrophosphatase and are essential
77 for decapping (4, 6). Except for the DCP2-DCP1 complex, Pat1 (Decapping activator
78 and translation repressor) (7-10), Dhh1 (Decapping activator and translation repressor)
79 (10-13) and the Lsm1-7 complex (Decapping activator) (10, 12, 14) are involved in
80 the decapping of mRNAs. At present, the decapping of retrovirus RNAs by the
81 DCP2-DCP1 complex has been well characterized (3, 4). However, the role of
82 DCP1-DCP2 complex in DNA virus infection remains unclear.
83 Although the DCP1-DCP2 complex affects the mRNA stability, the regulation of
84 DCP1-DCP2 complex mediated by microRNAs (miRNAs) has not been extensively
85 explored. During many eukaryotic cellular processes the miRNA pathway is essential,
86 in especial as virus-host interaction, development, apoptosis, immune response,
87 tumorigenesis and homeostasis (15-17). Primary miRNAs (pri-miRNAs) and
88 precursor-miRNAs (pre-miRNAs) are the essential steps of miRNAs in cell nucleus
89 (18-20). After being transported into cytoplasm, pre-miRNAs are processed by Dicer,
90 producing ~ 22 bp mature miRNA duplexes. The RNA-induced silencing complex
91 (RISC) is formed after the loading of the guiding strand of miRNA onto Argonaute
92 (Ago) protein (18). The target mRNA is bound to the miRNA and then it will be
93 cleaved by the Ago protein, in the RISC (18). Recently, it has been reported that
94 phosphorylation and dephosphorylation of Ago2 protein in human body have a
95 significant impact on the role of miRNA in RISC. (15). In the virus-host interactions,
96 the gene expressions can be regulated by host and/or virus miRNAs (20-31). In
97 shrimp, the host miRNAs expression are altered by the infection of white spot

98 syndrome virus (WSSV), a virus with a double-stranded DNA genome (25, 27, 30,
99 31). Shrimp miR-7 can target the WSSV early gene wsv477, thus inhibiting virus
100 infection (17), while a viral miRNA can target the shrimp caspase 8 gene to suppress
101 the host antiviral apoptosis (25). It has been reported that virus-originated mirnas
102 promote viral latency during viral infection through RNA editing (32). At present,
103 however, the influence of miRNA-mediated regulation of the DCP1-DCP2 complex
104 on virus infection remains to be investigated.

105 To address the influence of DCP1-DCP2 complex on DNA virus infection and the
106 role of the miRNA-regulated DCP1-DCP2 complex in virus infection, shrimp and
107 WSSV miRNAs targeting the DCP1-DCP2 complex were characterized in this study.
108 The results indicated that shrimp miR-87 and viral WSSV-miR-N46 (a viral miRNA)
109 could suppress virus infection by targeting the DCP1-DCP2 complex.

110 **Materials and methods**

111 **Shrimp culture and WSSV challenge**

112 Shrimp (*Marsupenaeus japonicus*), 10 to 12 cm in length, were cultured in groups
113 of 20 individuals in the tank filled with seawater at 25℃ (23). To ensure that shrimp
114 were virus-free before experiments, PCR using WSSV-specific primers (5'-TATTGT
115 CTC TCCTGACGTAC-3' and 5'-CACATTCTTCACGAGTCTAC-3') was
116 performed to detect WSSV in shrimp (23). The virus-free shrimp were infected with
117 WSSV inoculum (10^5 copies/ml) by injection at 100 μl/shrimp into the lateral area of
118 the fourth abdominal segment of shrimp (23). At different time postinfection, three
119 shrimp were randomly collected for each treatment. The shrimp hemocytes were
120 collected for later use.

121 **Analysis of WSSV copies with quantitative real-time PCR**

The genomic DNA of WSSV was extracted with a SQ tissue DNA kit (Omega Bio-tek, Norcross, GA, USA) according to the manufacturer's instruction. The extracted DNA was analyzed by quantitative real-time PCR with WSSV-specific primers and WSSV-specific TaqMan probe (5'-FAM-TGCTGCCGTCTCCAA -TAMRA-3') as described previously (Huang et al, 2014) (23). The PCR procedure was 95°C for 1 min, followed by 40 cycles of 95°C for 30 s, 52°C of 30 s, and 72°C for 30 s (23).

Detection of mRNA or miRNA by Northern blotting

The RNA was extracted from shrimp hemocytes with mirVana miRNA isolation kit (Ambion, USA). After separation on a denaturing 15% polyacrylamide gel containing 7M urea, the RNA was transferred to a Hybond-N+ nylon membrane, followed by ultraviolet cross-linking (23). The membrane was prehybridized in DIG (digoxigenin) Easy Hyb granule buffer (Roche, Basel, Switzerland) for 0.5 h at 42℃ and then hybridized with DIG-labeled miR-87 (5'-GAGGGGAAAAGCCATACGCT TA-3'), WSSV-miR-N46 (5'-AGUGCCAAGAUAACGGUUGAAG-3'), U6 (5'-GG GCCATGCTAATCTTCTCTGTATCGTT-3'), wsv477 (5'-CGAT TTCGGCAGGC CAGTTGTCAGA-3'), DCP2 (5'-CCAGAAACCCTGAACTAAGAGAA-3') or actin (5'-CTCGCTCGGCGGTGGTCGTGAAGG-3') probe at 42 ℃ overnight (23). Subsequently the detection was performed with the DIG High Prime DNA labeling and detection starter kit II (Roche).

Silencing or overexpression of miR-87 or WSSV-miR-N46 in shrimp

To knock down miR-87 or WSSV-miR-N46, an anti-miRNA oligonucleotide (AMO) was injected into WSSV-infected shrimp (23). AMO-miR-87 (5'-TGTACGTTTC TGGAGC-3') and AMO-WSSV-miR-N46

(5'-CTTCAACCGTTATCTTGGCACT -3') were synthesized (Sangon Biotech, Shanghai, China) with a phosphorothioate backbone and a 2'-O-methyl modification at the 12th nucleotide. AMO (10 nM) and WSSV (10^5 copies/ml) were co-injected into virus-free shrimp at a 100 μl/shrimp (23). At 16 h after the co-injection, AMO (10 nM) was injected into the same shrimp. As controls, AMO-miR-87-scrambled (5'-TTGCATGTCTGTCGAG-3'), AMO-WSSV- miR-N46-scrambled (5'-TTGCATGTCTGTCGAG-3'), WSSV alone (10^5 copies/ml) and phosphate buffered saline (PBS) were included in the injections. To overexpress miR-87 or WSSV-miR-N46, the synthesized miR-87 (5'-TAAGCGTAT GGCTTTTCCCCTC-3') (10 nM) or WSSV-miR-N46 (5'- AGTGCCAAGATAACG GTTGAAG-3') and WSSV (10^5 copies/ml) were co-injected into shrimp. As controls, miR-87-scrambled (5'-TATCGCATAGGCTTTTCCCCTC-3'), WSSV-miR-N46- scrambled (5'-ATTTGACAGATGCCTAGTACCAG-3'), WSSV alone (10^5 copies/ml) and PBS were used (23). The miRNAs were synthesized by Sangon Biotech (Shanghai, China).

At different time after treatment with AMO or miRNA, three shrimp were collected at random for each treatment. The shrimp hemocytes were collected for later use. At the same time, the cumulative mortality of shrimp was examined daily. All the experiments were biologically repeated three times.

Prediction of miRNA target genes

To predict the target genes of a miRNA, four independent computational algorithms including TargetScan 5.1 (http://www.targetscan.org), miRanda (http:// www. microrna.org/), Pictar (http://www.pictar.mdc-berlin.de/) and miRlnspector (http:/ /www.Imbb.Forth.gr/microinspector) were used (23). The overlapped genes predicted by the four algorithms were the potential targets of the miRNA.

Cell culture, transfection and fluorescence assays

171 Insect High Five cells (Invitrogen, USA) were cultured with Express Five
172 serum-free medium (Invitrogen) containing L-glutamine (Invitrogen) at 27℃ (23). To
173 determine the dosage of a synthesized miRNA, 10, 50, 100, 200, 500 or 1000 pM of
174 miRNA was transfected into cells (23). Then the miRNA expression in cells was
175 detected with quantitative real-time PCR. It was indicated that the transfection of
176 miRNA at 100 pM or more could overexpress miRNA in cells. The insect cells were
177 co-transfected with EGFP, EGFP-DCP2-3'UTR, EGFP-ΔDCP2-3'UTR,
178 EGFP-DCP1-3'UTR or EGFP-ΔDCP1-3'UTR and miRNA (miR-87 or
179 WSSV-miR-N46). All the miRNAs were synthesized by Shanghai GenePharma Co.,
180 Ltd (Shanghai, China). At 48h after co-transfection, the fluorescence intensity of cells
181 was evaluated with a Flex Station II microplate reader (Molecular Devices, USA)
182 at 490/510 nm excitation/emission (Ex/Em) (23). The experiments were biologically
183 repeated three times.

184 **Western blot analysis**

185 Shrimp tissues were homogenized with a lysis buffer (50 mM Tris-HCl, 150 mM
186 NaCl, 0.1% SDS, 1% Triton X-100, 1 mM phenylmethylsulfonyl fluoride, pH7.8) and
187 then centrifuged at 10,000×g for 10 min at 4°C. The proteins were separated by
188 12.5% SDS-polyacrylamide gel electrophoresis and then transferred onto a
189 nitrocellulose membrane. The membrane was blocked with 5% non-fat milk in TBST
190 (10 mM Tris-HCl, 150 mM NaCl, 20% Tween 20, pH7.5) for 2 h at room temperature,
191 followed by incubation overnight with a primary antibody. The antibodies were
192 prepared in our laboratory. After washes with TBST, the membrane was incubated
193 with horseradish peroxidase-conjugated secondary antibody (Bio-Rad, USA) for 2 h
194 at room temperature. Subsequently the membrane was detected using a Western
195 Lightning Plus-ECL kit (Perkin Elmer, USA).

196 **RNAi (RNA interference) assay in shrimp**

197 To silence gene expression in shrimp, RNAi assay was conducted. The small
198 interfering RNA (siRNA) specifically targeting the *DCP1* or *DCP2* gene was
199 designed with the 3' UTR of the *DCP1* or *DCP2* gene, generating DCP1-siRNA (5'-A
200 AUCGCAGUUGCUAUGCGUUGGACG-3') or DCP2-siRNA (5'-GCGGAAGAC
201 CGUGCCCGUAAUAUAA-3'). As a control, the sequence of DCP1-siRNA or
202 DCP2-siRNA was randomly scrambled (DCP1-siRNA-scrambled, 5'-GACAUUAAG
203 AUAUAUAUGG-3'; DCP2-siRNA-scrambled, 5'-CGCCUUCUGGCACGGGCAU
204 UAUAUU-3'). All the siRNAs were synthesized by the in vitro transcription T7 kit
205 (TaKaRa, Japan) according to the manufacturer's instructions. The synthesized
206 siRNAs were quantified by spectrophotometry. The shrimp were co-injected with
207 WSSV (10^4 copies/shrimp) and siRNA (4nM). PBS and WSSV alone (10^4
208 copies/shrimp) were included in the injections as controls (23). At 0, 24, 36 and
209 48 h after infection, the hemocytes of three shrimp, randomly selected from each
210 treatment, were collected for later use. At the same time, the cumulative mortality of
211 shrimp was examined daily (23). All the experiments were biologically repeated three
212 times.

213 **Co-immunoprecipitation**

214 Shrimp hemocytes were lysed with ice-cold cell lysis buffer (Beyotime). Then the
215 lysate was incubated with Protein G-agarose beads (Invitrogen, Carlsbad, CA, USA)
216 for 2h at room temperature, followed by incubation with DCP2-specific antibody
217 overnight at 4^0C. After washes three times with ice-cold lysis buffer, the
218 immuno-complex was subjected to SDS-PAGE with Coomassie blue staining. The
219 proteins were identified with mass spectrometry using a Reflex IV MALDI-TOF mass
220 spectrometer (Bruker Daltonik, Bremen, USA). The spectra were processed by the

Xmass software (Bruker Daltonik, Bremen) and the peak lists of the mass spectra were used for peptide mass fingerprint analyses with the Mascot software (Matrix Science).

Cloning of full-length cDNAs of shrimp *DCP1* and *DCP2* gene

The full-length *DCP1* and *DCP2* cDNAs were obtained by rapid amplification of cDNA ends (RACE) using a 5'/3' RACE kit (Roche, Indianapolis, IN, USA). RACEs were conducted according to the manufacturer's instructions using DCP1-specific primers (5'RACE, 5'-CCTGGGACACTTGAAG-3' and 5'-GGGTAAACCAGTGCC -3'; 3'RACE, 5'-GCCCCACAGTCCCACCCACCT-3' and 5'-CCCAGGAGGAGCA CCAATCTCA-3') or DCP2-specific primers (5'RACE, 5'-GGGAACCATTTCAGT TGCT-3' and 5'-GCCAGAAACCCTGAACTAAG-3'; 3'RACE, 5'-ATTGGAGAGC AGTTTGTGAGAC-3' and 5'-TTTACATCATCCCAGGCG-3'). PCR products were cloned into pMD-19 vector (Takara, Japan) and sequenced.

Interactions between DCP1 and DCP2 domains

To explore the interaction between DCP1 and DCP2 proteins, the full-length and domain deletion mutants of DCP1 and DCP2 were cloned into pIZ/EGFP V5-FLAG and pIZ/EGFP V5-His (Invitrogen, USA), respectively. The full-length and deletion mutants of DCP1 and DCP2 were amplified by PCR with sequence-specific primers (full-length DCP1, 5'-GGAAGATCTATGCGCTAAGGTTTTATTTGGAAAAA -3' and 5'-CCGCTCGAGTGACTTATCGTCGTCATCCTTGTAATCCAAACAAC CTTTGATAGAGAGAT-3'; DCP1 EVH1 domain, 5'-GGAAGATCTATGCGCTA AGGTTTTATTTGGAAAAA-3' and 5'-CCGCTCGAGTGACTTATCGTCGTCATC CTTGTAATCTATGTCCCCTCCAGGTGCCCCA-3'; DCP1 C-terminal extension region, 5'-GGAAGATCTGAATGACAAATCAAGTGA-3' and 5'-CCGCTCGAG TGACTTATCGTCGTCATCCTTGTAATCCAAACAACCTTTGATAGAGAGAT -3'; full-length DCP2, 5'-GGAAGATCTATGGCCCCACCAACAGGTGGAAAA

-3' and 5'-TCCCCGCGGTTAATGGTGATGGTGATGATGCCAAGACAGCATC ACATCGGCCC-3'; DCP2 N-regulatory domain, 5'-CGCGGATCCGATGAAGA ACCACATTGTTGTGCC-3' and 5'-TCCCCGCGGTTAATGGTGATGGTGATG ATGCCAAGACAGCATCACATCGGCCC-3'; DCP2 C-terminal divergent region, 5'-CGCGGATCCGATGAAGAACCACATTGTTGTGCC-3' and 5'-TCCCCGCGG TTAATGGTGATGGTGATGATGCTGGCGGTCAGAGGTACTGGTG-3'; DCP2 Nudix domain, 5'-CG CGGATCCATGGCCCCACCAACAGGTGGAAAA-3' and 5'-TCCCCGCGGCACATTAATTTTCCCTTTTGG-3', and 5'-TCCCCGCGGATGG CCCCACCAACAGGTGGAAAA-3' and 5'-TCCCCGCGGTTAATGGTGATGGTG ATGA TGCCAAGA CAGCATCACATCGGCCC-3').

The constructs were co-transfected into insect High Five cells at 70% confluence using Cellfectin transfection reagent (Invitrogen, USA) according to the manufacturer's protocol. The cells were cultured at 27 ℃ in Express Five serum-free medium (Invitrogen) supplemented with L-glutamine (Invitrogen). At 48 h after co-transfection, the cells were subjected to immunoprecipitation assays with anti-His or anti-FLAG antibody, followed by Western blot analysis.

Statistical analysis

All the numerical data presented were analyzed by one-way analysis of variance (ANOVA) to calculate the means and standard deviations of triplicate assays.

Results

Role of shrimp DCP2 in virus infection

To characterize the role of shrimp DCP2 in virus infection, the expression level of DCP2 was examined in shrimp in response to WSSV infection. The results indicated

that DCP2 was significantly upregulated in virus-challenged shrimp (Fig 1A), suggesting that DCP2 played an important role in virus infection.

To explore the influence of DCP2 silencing on virus infection, the DCP2 expression was knocked down by sequence-specific DCP2-siRNA in shrimp (Fig 1B). The results revealed that the DCP2 silencing resulted in significant decreases of WSSV copies compared with the controls (Fig 1C), showing that DCP2 played an essential role in WSSV infection.

Proteins interacted with DCP2

To elucidate the mechanism of DCP2-mediated antiviral immunity in shrimp, the proteins interacted with DCP2 were characterized. The results of co-immunoprecipitation assays using shrimp DCP2-specific antibody indicated that two proteins were obtained compared with the control (Fig 2A). Mass spectrometry identification revealed that the two proteins were DCP1 and DCP2 (Fig 2A). These data showed that DCP2 was interacted with DCP1 in shrimp. To confirm the interaction between DCP1 and DCP2 proteins, the plasmids expressing DCP1 and DCP2 were co-transfected into insect cells, followed by Co-IP using DCP2-specific antibody. Western blots revealed that the DCP1 protein was directly interacted with the DCP2 protein (Fig 2B).

To identify which domains of DCP1 and DCP2 were interacted, the deletion mutants of DCP1 EVH1 domain (ΔEVH1, FLAG-tagged), DCP1 C-terminal region (ΔCR, FLAG-tagged), DCP2 N-terminal regulatory domain (ΔNRD, His-tagged), DCP2 Nudix domain (ΔND, His-tagged) and DCP2 C-terminal divergent region (ΔCDR, His-tagged) were constructed, respectively (Fig 2C). The deletion constructs and the full-length DCP1 (FLAG-tagged) or DCP2 (His-tagged) were co-transfected into insect cells. The results showed that when insect cells were co-transfected with

295 DCP2 ΔNRD and full-length DCP1, the DCP1 protein was not detected in the
296 immunoprecipitated product using His antibody (Fig 2D), showing that DCP1 was
297 interacted with DCP2 N-terminal regulatory domain. When DCP2 and DCP1 ΔEVH1
298 were co-transfected into cells, the DCP2 protein did not exist in the
299 immunoprecipitated complex (Fig 2E), indicating that DCP2 was interacted with
300 DCP1 by binding to its EVH1 domain.

301 The above findings indicated that the EVH1 domain of DCP1 was interacted with
302 the N-terminal regulatory domain of DCP2.

303 **Role of shrimp DCP1 in virus infection**

304 To explore the influence of DCP1 on virus infection of shrimp, the expression
305 profile of DCP1 was examined in hemocytes of WSSV-infected shrimp. The data of
306 Northern blots and Western blots indicated that the DCP1 expression was
307 significantly upregulated in shrimp in response to WSSV infection, suggesting the
308 involvement of DCP1 in virus infection (Fig 3A).

309 In an attempt to assess the role of DCP1 in virus infection, the DCP1 expression
310 was knocked down by sequence-specific siRNA in WSSV-infected shrimp, followed
311 by evaluation of virus infection. The results revealed that the expression of DCP1 was
312 silenced by DCP1-siRNA (Fig 3B). The DCP1 silencing led to significant decreases
313 of WSSV copies compared with the controls (WSSV and WSSV+DCP1-siRNA-
314 scrambled) (Fig 3C). These findings indicated that DCP1 played a positive role in
315 virus infection.

316 **Effects of the interaction between shrimp miR-87 and *DCP2* on virus infection**

317 To reveal the miRNAs targeting shrimp *DCP2* gene, the miRNAs targeting *DCP2*
318 were predicted. The prediction data showed that the shrimp *DCP2* gene was a
319 potential target of miR-87 (Fig 4A). To evaluate the interaction between miR-87 and

320 *DCP2* gene, the plasmid pIZ/EGFP-DCP2-3'UTR containing the EGFP and
321 the DCP2 3'UTR was co-transfected with miR-87 into the insect cells. The results
322 indicated that the fluorescence intensity of the cells co-transfected with miR-87 and
323 pIZ/EGFP-DCP2-3'UTR was significantly decreased compared with the controls (Fig
324 4B). However, the fluorescence intensity of the cells co-transfected with miR-87 and
325 EGFP-ΔDCP2-3'UTR was similar to those of the controls (Fig 4B).
326 These findings revealed that miR-87 was directly interacted with *DCP2* gene. In order
327 to examine the interaction between miR-87 and *DCP2* gene *in vivo*, miR-87 was
328 overexpressed in shrimp, followed by the analysis of *DCP2* gene expression. It
329 was revealed that the miR-87 overexpression led to a significant decrease of *DCP2*
330 expression at transcript and protein levels compared with the controls (Fig 4C),
331 indicating that miR-87 was interacted with *DCP2* gene *in vivo*.

332 To explore the role of shrimp miR-87 in virus infection of shrimp, the expression
333 level of miR-87 was examined in hemocytes of WSSV-infected shrimp. Northern
334 blots indicated that the host miR-87 expression was significantly downregulated in
335 shrimp in response to WSSV infection, suggesting that miR-87 played an important
336 role in the shrimp antiviral immunity (Fig 4D).

337 In order to assess the influence of miR-87 on virus infection, the miR-87
338 expression was silenced or overexpressed in the WSSV-infected shrimp, followed by
339 the evaluation of virus infection. The results showed that the expression of miR-87
340 was knocked down by AMO-miR-87 compared with the controls (Fig 4E). The
341 miR-87 silencing led to significant increases of WSSV copies and the virus-infected
342 shrimp mortality compared with the controls (Fig 4F and 4G). On the other hand,
343 when miR-87 was overexpressed (Fig4H), the WSSV copies and the virus-infected

shrimp mortality were significantly decreased compared with the controls (Fig 4G and 4I).

Taken the above data together, these findings presented that miR-87 could inhibit virus infection in shrimp by targeting shrimp *DCP2* gene.

Influence of viral WSSV-miR-N46 targeting *DCP1* on virus infection

To characterize the miRNAs targeting *DCP1*, the viral miRNAs targeting *DCP1* gene were predicted. The miRNA target prediction showed that the *DCP1* gene might be the target of WSSV-miR-N46, a viral miRNA encoded by WSSV (Fig 5A). To validate the target prediction, the synthesized viral miRNA and the plasmid EGFP-DCP1-3' UTR were co-transfected into insect cells. The results indicated that the fluorescence intensity of the cells co-transfected with WSSV-miR-N46 and EGFP-DCP1-3' UTR was significantly decreased compared with that in the controls (Fig 5B), showing that WSSV-miR-N46 was directly interacted with *DCP1* gene.

In an attempt to reveal the role of WSSV-miR-N46 in virus infection, the expression of WSSV-miR-N46 in WSSV-challenged shrimp was examined. Northern blotting results indicated that WSSV-miR-N46 was detected at 48 h after virus infection in shrimp (Fig 5C). Therefore, WSSV-miR-N46 was overexpressed in shrimp (Fig 5D), followed by evaluation of virus copy. The results revealed that the WSSV-miR-N46 overexpression significantly decreased the number of WSSV copies in shrimp (Fig 5E), indicating that WSSV-miR-N46 played a negative role in WSSV replication.

Taken together, the findings revealed that the viral miRNA (WSSV-miR-N46) and host miRNA (miR-87) suppressed virus infection by targeting the DCP1-DCP2 complex (Fig 5F).

Discussion

As reported, the DCP1-DCP2 complex, localized in processing bodies (P bodies), can regulate the animal antiviral immunity by two strategies, that is the decapping of retrovirus RNAs and the suppression of RNAi pathway (32-36). During the process of retrovirus infection, the canonical mRNA decapping enzyme DCP2, along with its activator DCP1, could restrict the infection of retrovirus at the level of mRNA transcription (34, 35). The host DCP1-DCP2 complex directly decapps retrovirus mRNAs or cellular mRNAs targeted by bunyaviruses for cap-snatching, thus creating a bottleneck for retrovirus replication (33, 35). During the infection of Sindbis virus or Venezuelan equine encephalitis virus, the host can inhibit the infection of retrovirus through the DCP1-DCP2-mediated 5'-3' decay pathway. During the bunyaviruses infection in the insects and mammals, the bunyaviruses cap their mRNAs at the 5' ends by the "cap-snatching" machinery in the P bodies (35). The virally encoded nucleocapsid N protein recognize 5' caps and 10-18 nucleotides (nt) downstream 5' caps of cellular mRNAs and the viral RNA-dependent RNA polymerase cleaves the mRNA at the same position. Subsequently the cleaved 5' caps are used for viral mRNA synthesis (35). Regarding the role of the DCP2-DCP2 complex in RNAi pathway, it is found that the silencing of DCP2 and/or DCP1 promotes RNAi, showing that the DCP2-DCP1 complex takes a negative effect on the RNAi pathway (35, 36). RNAi, an important component of innate immune responses, mediated by siRNAs or miRNAs, plays crucial roles against virus infection in invertebrates and plants that rely solely on innate mechanisms to combat viral infection (30, 34, 37). Up to date, however, little is known about the role of the DCP1-DCP2 complex in DNA virus infection. In the present study, the findings indicated that the silencing of the DCP1-DCP2 complex inhibited the infection of WSSV, a DNA virus of shrimp, suggesting that the DCP1-DCP2 complex facilitated DNA virus infection. Due to the

394 suppressive role of the DCP1-DCP2 complex in RNAi pathway against virus
395 infection (35, 36), the DCP1-DCP2 complex could promote WSSV infection in
396 shrimp. In this context, our study contributed a novel aspect of the DCP1-DCP2
397 complex in virus-host interactions.

398 In the present investigation, the results showed that the host and viral miRNAs
399 could inhibit the expressions of DCP1 and DCP2 during DNA virus infection.
400 MiRNAs, a large class of small noncoding RNAs in diverse eukaryotic organisms, are
401 sequentially processed by two RNase III proteins, Drosha and Dicer from the stem
402 regions of long hairpin transcripts (28, 37). The mature miRNA strand is liberated
403 from the miRNA:miRNA* duplex and integrated into the RNA induced silencing
404 complex (RISC), and inhibits the expression of cognate mRNA through degradation
405 or translation repression in the RISC (18). During virus infection the host miRNAs
406 or/and viral miRNAs can regulate virus infection by targeting viral or/and host genes
407 (2, 17, 23, 24, 27-29, 31, 32, 38). As well reported, the virus-encoded miRNAs (viral
408 mRNAs) can target virus and/or host genes, leading to virus infection or virus latency
409 (29, 32, 38, 39). In shrimp, a viral miRNA WSSV-miR-N12 targets the
410 virus wsv399 gene, resulting in virus latency (32). The viral miRNA-mediated
411 regulation of virus infection or virus latency is an efficient strategy for virus to escape
412 its host immune responses. However, the involvement of miRNA in the degradation
413 of cellular mRNAs mediated by DCP1-DCP2 complex has not been explored. Our
414 study revealed that the host and viral miRNAs could regulate the DCP1-DCP2
415 complex to affect virus infection. Therefore, our study provided novel insights into
416 the regulatory mechanism of DCP1-DCP2 complex in virus-host interactions and that
417 the miRNA-mediated regulation of DCP1-DCP2 complex took great effects on RNAi
418 immunity of invertebrates against virus infection.

Acknowledgements

This work was supported by National Natural Science Foundation of China (31430089) and National Program on the Key Basic Research Project (2015CB755903).

References:

1. Bhattacharjee S, Chattaraj S. 2017. Entry, infection, replication, and egress of human polyomaviruses: an update. Can J Microbiol 63: 193-211.

2. Cui Y, Huang X, Wang X, Li Y, Tang C, Wang H, Jiang Y. 2017. Correlation between infection of herpes virus family and liver function parameters: a population-based cross-sectional study. J Infect Dev Ctries 11: 320-325.

3. Rossi JJ. 2005. RNAi and the P-body connection. Nat Cell Biol 7: 643-644.

441 4. Chen CY, Zheng D, Xia Z, Shyu AB. 2009. Ago-TNRC6 triggers
442 microRNA-mediated decay by promoting two deadenylation steps. Nat Struct Mol
443 Biol 16: 1160–1166

444 5. Schaeffer D, van Hoof A. 2011. Different nuclease requirements for
445 exosome-mediated degradation of normal and nonstop mRNAs. Proc Natl Acad Sci U
446 S A 108: 2366-2371.

447 6. Munchel SE, Shultzaberger RK, Takizawa N, Weis K. 2011. Dynamic profiling of
448 mRNA turnover reveals gene-specific and system-wide regulation of mRNA decay.
449 Mol Biol Cell 22: 2787-2795.

450 7. Eulalio A, Behm-Ansmant I, Schweizer D, Izaurralde E. 2007. P-body formation is
451 a consequence, not the cause, of RNA-mediated gene silencing. Mol Cell Biol 27:
452 3970-3981.

453 8. Gallo CM, Munro E, Rasoloson D, Merritt C, Seydoux G. 2008. Processing bodies
454 and germ granules are distinct RNA granules that interact in C. elegans embryos. Dev
455 Biol 323: 76-87.

456 9. Scheller N, Resa-Infante P, de la Luna S, Galao RP, Albrecht M, Kaestner L, Lipp
457 P, Lengauer T, Meyerhans A, Diez J. 2007. Identification of PatL1, a human homolog
458 to yeast P body component Pat1. Biochim Biophys Acta 1773: 1786-1792.

459 10. Sheth U, Parker R. 2003. Decapping and decay of messenger RNA occur in
460 cytoplasmic processing bodies. Science 300: 805-808.

461 11. Barbee SA, Estes PS, Cziko AM, Hillebrand J, Luedeman RA, Coller JM, Johnson
462 N, Howlett IC, Geng C, Ueda R, Brand AH, Newbury SF, Wilhelm JE, Levine RB,
463 Nakamura A, Parker R, Ramaswami M. 2006. Staufen- and FMRP-containing neuronal

464 RNPs are structurally and functionally related to somatic P bodies. Neuron 52:
465 997-1009.

466 12. Gallo RL, Nizet V. 2008. Innate barriers against infection and associated disorders.
467 Drug Discov Today Dis Mech 5: 145-152.

468 13. Wilczynska U, Szymczak W, Szeszenia-Dabrowska N. 2005. Mortality from
469 malignant neoplasms among workers of an asbestos processing plant in Poland:
470 results of prolonged observation. Int J Occup Med Environ Health 18: 313-326.

471 14. Stoecklin G, Mayo T, Anderson P. 2006. ARE-mRNA degradation requires the
472 5'-3' decay pathway. EMBO Rep 7: 72-77.

473 15. Golden RJ, Chen B, Li T, Braun J, Manjunath H, Chen X, Wu J, Schmid V, Chang
474 TC, Kopp F, Ramirez-Martinez A, Tagliabracci VS, Chen ZJ, Xie Y, Mendell JT. 2017.
475 An Argonaute phosphorylation cycle promotes microRNA-mediated silencing. Nature
476 542: 197-202.

477 16. Jo MH, Shin S, Jung SR, Kim E, Song JJ, Hohng S. 2015. Human Argonaute 2 Has
478 Diverse Reaction Pathways on Target RNAs. Mol Cell 59: 117-124.

479 17. Huang T, Zhang X. 2012. Functional analysis of a crustacean microRNA in
480 host-virus interactions. J Virol 86: 12997-13004.

481 18. Jonas S, Izaurralde E. 2015. Towards a molecular understanding of
482 microRNA-mediated gene silencing. Nat Rev Genet 16: 421-433.

483 19. Vidigal JA, Ventura A. 2015. The biological functions of miRNAs: lessons from in
484 vivo studies. Trends Cell Biol 25: 137-147.

485 20. Yang G, Yang L, Zhao Z, Wang J, Zhang X. 2012. Signature miRNAs involved in
486 the innate immunity of invertebrates. PLoS ONE 7: e39015.

487 21. Mendell JT, Olson EN. 2012. MicroRNAs in stress signaling and human disease.
488 Cell 148: 1172-1187.

489 22. Zhou Y, He Y, Wang C, Zhang X. 2015. Characterization of miRNAs from
490 hydrothermal vent shrimp Rimicaris exoculata. Mar Genomics 24 Pt 3: 371-378.

491 23. He Y, Zhang X. 2012. Comprehensive characterization of viral miRNAs involved
492 in white spot syndrome virus (WSSV) infection. RNA Biol 9: 1019-1029.

493 24. Huang T, Cui Y, Zhang X. 2018. Correction for Huang et al., "Involvement of
494 Viral MicroRNA in the Regulation of Antiviral Apoptosis in Shrimp". J Virol 92.

495 25. Wang Z, Zhu F. 2017. MicroRNA-100 is involved in shrimp immune response to
496 white spot syndrome virus (WSSV) and Vibrio alginolyticus infection. Sci Rep 7:
497 42334.

498 26. Ingle H, Kumar S, Raut AA, Mishra A, Kulkarni DD, Kameyama T, Takaoka A,
499 Akira S, Kumar H. 2015. The microRNA miR-485 targets host and influenza virus
500 transcripts to regulate antiviral immunity and restrict viral replication. Sci Signal 8:
501 a126.

502 27. Shu L, Li C, Zhang X. 2016. The role of shrimp miR-965 in virus infection. Fish
503 Shellfish Immunol 54: 427-434.

504 28. Ren Q, Huang X, Cui Y, Sun J, Wang W, Zhang X. 2017. Two white spot
505 syndrome virus microRNAs target the dorsal gene to promote virus infection in

506 *Marsupenaeus japonicus* shrimp. J Virol 91 (8): e02261-16. https://doi.org/
507 10.1128/JVI. 02261-16.

508 29. He Y, Yang K, Zhang X. 2014. Viral microRNAs targeting virus genes promote
509 virus infection in shrimp in vivo. J Virol 88: 1104-1112.

510 30. Huang T, Xu D, Zhang X. 2012. Characterization of host microRNAs that respond
511 to DNA virus infection in a crustacean. BMC Genomics 13: 159.

512 31. Cui Y, Yang X, Zhang X. 2017. Shrimp miR-34 from Shrimp Stress Response to
513 Virus Infection Suppresses Tumorigenesis of Breast Cancer. Mol Ther Nucleic Acids 9:
514 387-398.

515 32. Cui Y, Huang T, Zhang X. 2015. RNA editing of microRNA prevents
516 RNA-induced silencing complex recognition of target mRNA. Open Biol 5: 150126.

517 33. Gaglia MM, Glaunsinger BA. 2010. Viruses and the cellular RNA decay
518 machinery. Wiley Interdiscip Rev RNA 1: 47-59.

519 34. Hopkins KC, McLane LM, Maqbool T, Panda D, Gordesky-Gold B, Cherry S.
520 2013. A genome-wide RNAi screen reveals that mRNA decapping restricts bunyaviral
521 replication by limiting the pools of Dcp2-accessible targets for cap-snatching. Genes
522 Dev 27: 1511-1525.

523 35. Hopkins K, Cherry S. 2013. Bunyaviral cap-snatching vs. decapping: recycling
524 cell cycle mRNAs. Cell Cycle 12: 3711-3712.

525 36. Sheth U, Parker R. 2006. Targeting of aberrant mRNAs to cytoplasmic processing
526 bodies. Cell 125: 1095-1109.

527 37. Huang T, Zhang X. 2012. Contribution of the argonaute-1 isoforms to invertebrate
528 antiviral defense. PLoS ONE 7: e50581.

529 38. He Y, Ma T, Zhang X. 2017. The Mechanism of Synchronous Precise Regulation
530 of Two Shrimp White Spot Syndrome Virus Targets by a Viral MicroRNA. Front
531 Immunol 8: 1546.

532 39. He Y, Ma T, Zhang X. 2017. The Mechanism of Synchronous Precise Regulation
533 of Two Shrimp White Spot Syndrome Virus Targets by a Viral MicroRNA. Front
534 Immunol 8: 1546.

535
536
537
538
539
540
541
542
543

544 **Figure legends**

545 **Fig 1. Role of shrimp DCP2 in virus infection.** (A) Expression level of DCP2 in
546 shrimp in response to virus infection. Shrimp were challenged with WSSV. At
547 different times post-infection, the expression level of DCP2 in shrimp hemocytes was
548 examined by Northern blotting or Western blotting. Shrimp β-actin was used as a
549 control. Numbers indicated the time post-infection. Probes or antibodies used were
550 shown on the left. (B) Knockdown of DCP2 by siRNA in shrimp. Shrimp were

551 injected with DCP2-siRNA to silence DCP2 expression. As a control, DCP2-siRNA-
552 scrambled was included in the injection. At different time after injection,
553 the *DCP2* mRNA and protein levels were examined by Northern blot and Western
554 blot, respectively. Actin was used as a control. The probes or antibodies were
555 indicated on the left. (C) Influence of DCP2 silencing on virus infection in shrimp.
556 Shrimp were co-injected with DCP2-siRNA and WSSV. At different time
557 post-infection, the WSSV copies were examined with quantitative real-time PCR (*,
558 $p< 0.05$; **, $p< 0.01$).

559 **Fig 2. Proteins interacted with DCP2.** (A) The proteins bound to
560 DCP2. Co-IP using the DCP2-specific antibody was conducted. The eluted proteins
561 were subjected to SDS-PAGE, followed by protein identification using mass
562 spectrometry. (B) The interaction between DCP1 and DCP2 proteins. The His-tagged
563 DCP1 and DCP2 were co-transfected into insect cells. At 48 h after
564 co-transfection, Co-IP was conducted using DCP2-specific antibody, followed by
565 Western blot analysis with anti-His IgG. (C) The constructs of DCP1 and DCP2
566 domain deletion mutants. (D) and (E) The interactions between DCP1 and DCP2
567 domains. The full-length and/or deletion mutants of DCP1 and DCP2 were
568 co-transfected into insect cells. At 48 h after transfection, the target proteins were
569 immunoprecipitated with anti-His (D) or anti-FLAG IgG (E), followed by Western
570 blot analysis.

571 **Fig 3. Role of shrimp DCP1 in virus infection.** (A) DCP1 expression profile in
572 shrimp in response to virus infection. Shrimp were challenged with WSSV. At
573 different times post-infection, the expression of DCP1 was examined in shrimp
574 hemocytes by Northern blotting or Western blotting. Shrimp β-actin was used as a
575 control. The numbers indicated the time post-infection. Probes or antibodies used

were shown on the left. (B) Silencing of DCP1 in shrimp. Shrimp were injected with DCP1-siRNA, followed by the detection of DCP1 with Northern blot or Western blot. The probes or antibodies were indicated on the left. (C) Influence of DCP1 silencing on virus infection. WSSV and DCP1-siRNA or DCP1-siRNA-scrambled were co-injected into shrimp. WSSV alone and PBS were used as controls. At different time after injection, the WSSV copies in shrimp were examined with quantitative real-time PCR (*, $p<0.05$; **, $p<0.01$).

Fig 4. Effects of the interaction between shrimp miR-87 and *DCP2* on virus infection. (A) Prediction of miRNAs targeting *DCP2*. According to the prediction, the 3' UTR of *DCP2* gene could be targeted by miR-87. The seed sequence of miR-87 was underlined. (B) Direct interaction between miR-87 and DCP2 3' UTR. The insect High Five cells were co-transfected with miR-87 and the plasmid EGFP-DCP2-3'UTR or EGFP-ΔDCP2-3'UTR. At 36 h after co-transfection, the fluorescence intensity of insect cells was evaluated. Scale bar, 50 μm. (C) Interaction between miR-87 and DCP2 *in vivo*. MiR-87 was overexpressed in shrimp. At different time after miR-87 overexpression, the *DCP2* mRNA and protein levels were examined by Northern blot and Western blot, respectively. As a control, miR-87-scrambled was included in the assays. Data were representatives of three independent experiments. The probes or antibodies were indicated on the left. (D) Expression level of miR-87 in virus-infected shrimp. Shrimp were challenged with WSSV. At different time post-infection, miR-87 was detected in hemocytes of virus-infected shrimp by Northern blotting. U6 was used as a control. Probes were indicated on the left. (E) Silencing of miR-87 expression in shrimp. Shrimp were co-injected with AMO-miR-87 and WSSV. As a control, AMO-miR-87-scrambled was included in the injection. At different time post-infection, miR-87 was detected

by Northern blot. The probes used were indicated on the left. The numbers showed the time points post-infection. U6 was used as a control. (F) Influence of miR-87 silencing on virus copies. WSSV and AMO-miR-87 or AMO-miR-87-scrambled were co-injected into shrimp. WSSV and PBS were used as controls. At different time after injection, the WSSV copies in shrimp were examined with quantitative real-time PCR. (G) Effects of miR-87 silencing or overexpression on WSSV-infected shrimp mortality. (H) Overexpression of miR-87 in shrimp. Shrimp were co-injected with miR-87 or miR-87-scrambled and WSSV. At different time after injection, the shrimp were subjected to Northern blot with probes indicated on the left. PBS and WSSV were used as controls. (I) Impact of miR-87 overexpression on WSSV copies. Shrimp were simultaneously injected with miR-87 and WSSV. As a control, miR-87-scrambled was included in the injection. At different time post-infection, the virus copies were examined with quantitative real-time PCR. In all panels, the significant differences between treatments were indicated (*, $p< 0.05$; **, $p< 0.01$).

Fig 5. Influence of viral WSSV-miR-N46 targeting *DCP1* on virus infection. (A) The prediction of viral miRNA targeting *DCP1*. As predicted, the 3' UTR of *DCP1* was targeted by WSSV-miR-N46, a WSSV-encoded viral miRNA. The seed sequence was underlined. (B) The direct interaction between WSSV-miR-N46 and *DCP1* gene in insect cells. Insect High Five cells were co-transfected with WSSV-miR-N46 or WSSV-miR-N46-scrambled and EGFP, EGFP-DCP1 3' UTR or EGFP-ΔDCP1 3' UTR. At 48 h after co-transfection, the fluorescence of cells was examined (**, $p<0.01$). Scale bar, 50 μm. (C) The expression pattern of WSSV-miR-N46 in shrimp in response to virus infection. Shrimp were challenged with WSSV. At different time post-infection, WSSV-miR-N46 was detected by Northern blotting. U6 was used as a

control. The number indicated the time points post-infection. Probes were indicated on the left. (D) The overexpression of WSSV-miR-N46 in shrimp. Shrimp were simultaneously injected with WSSV and WSSV-miR-N46. As a control, WSSV-miR-N46-scrambled was included in the injection. At different time post-infection, shrimp hemolymph was subjected to Northern blotting. U6 was used as a control. The probes were shown on the right. (E) The influence of WSSV-miR-N46 overexpression on WSSV infection. Shrimp were simultaneously injected with WSSV-miR-N46 and WSSV. As a control, WSSV-miR-N46-scrambled was included in the injection. At different time post-infection, the WSSV copies were examined with quantitative real-time PCR (**, $p<0.01$). (F) Mode for the miRNA-mediated signaling pathway in virus infection.

Fig 1

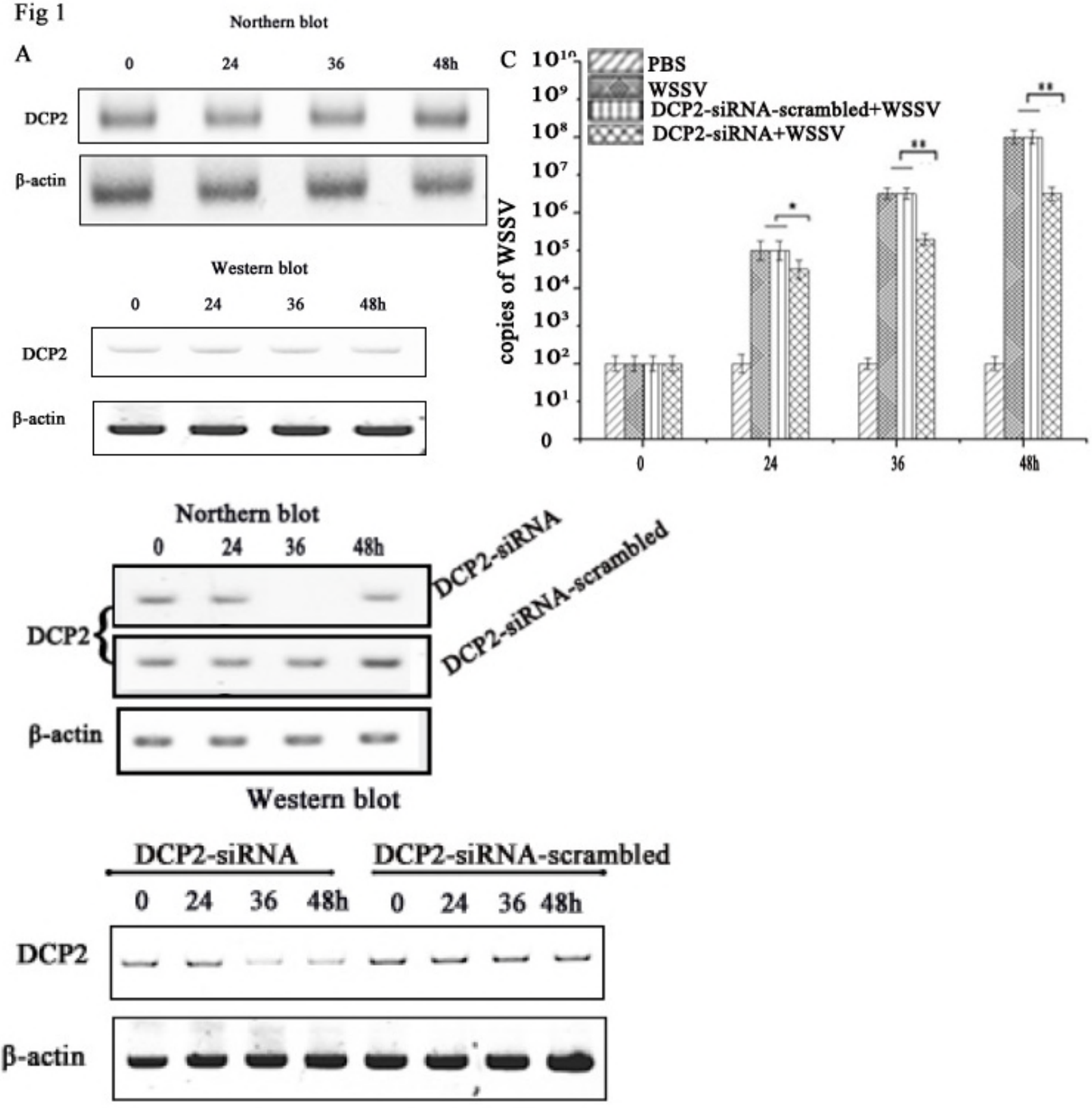
A
Northern blot
0
24
36
48h
DCP2
β-actin
Western blot
0
24
36
48h
DCP2
β-actin
C
PBS
WSSV
DCP2-siRNA-scrambled+WSSV
DCP2-siRNA+WSSV
copies of WSSV
0
24
36
48h
Northern blot
0
24
36
48h
DCP2-siRNA
DCP2-siRNA-scrambled
DCP2
β-actin
Western blot
DCP2-siRNA
DCP2-siRNA-scrambled
0
24
36
48h
0
24
36
48h
DCP2
β-actin

Fig 2

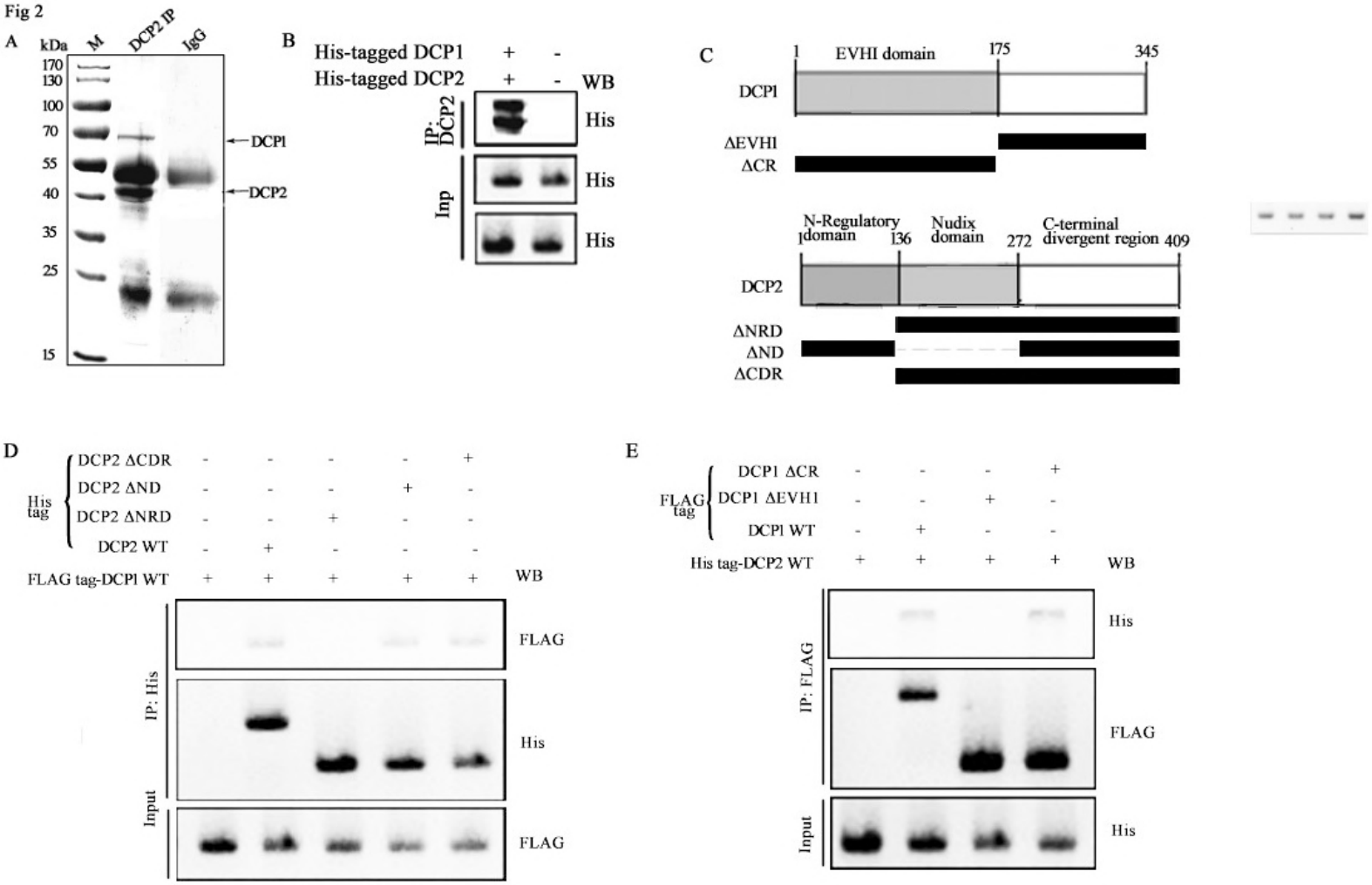
A
kDa
M
DCP2 IP
IgG
170
130
100
70
55
40
35
25
15
DCP1
DCP2
B
His-tagged DCP1 + -
His-tagged DCP2 + - WB
IP: DCP2
His
Inp
His
His
C
1
EVHI domain
175
345
DCP1
ΔEVH1
ΔCR
N-Regulatory domain
1
136
Nudix domain
272
C-terminal divergent region
409
DCP2
ΔNRD
ΔND
ΔCDR
D
His tag
DCP2 ΔCDR - - - - +
DCP2 ΔND - - - + -
DCP2 WT - + - - -
FLAG tag-DCP1 WT + + + + + WB
IP: His
FLAG
His
Input
FLAG
E
FLAG tag
DCP1 ΔCR - - - +
DCP1 ΔEVH1 - - + -
DCP1 WT - + - -
His tag-DCP2 WT + + + + WB
IP: FLAG
His
FLAG
Input
His

Fig 3

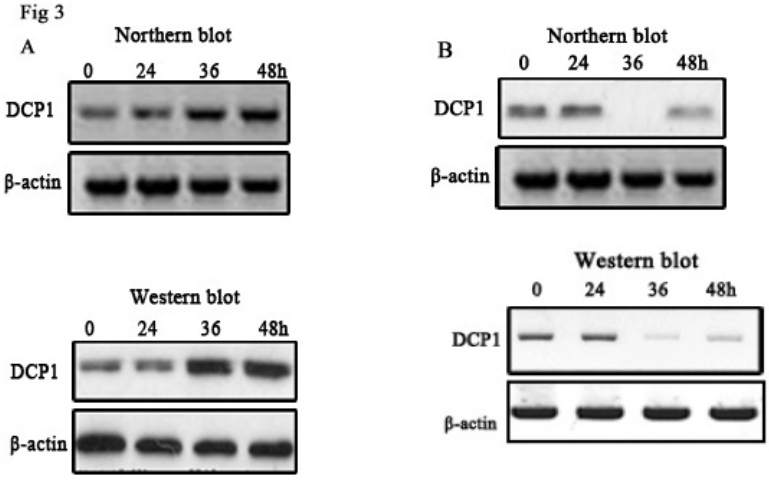
A
Northern blot
0 24 36 48h
DCP1
β-actin
B
Northern blot
0 24 36 48h
DCP1
β-actin
Western blot
0 24 36 48h
DCP1
β-actin
Western blot
0 24 36 48h
DCP1
β-actin

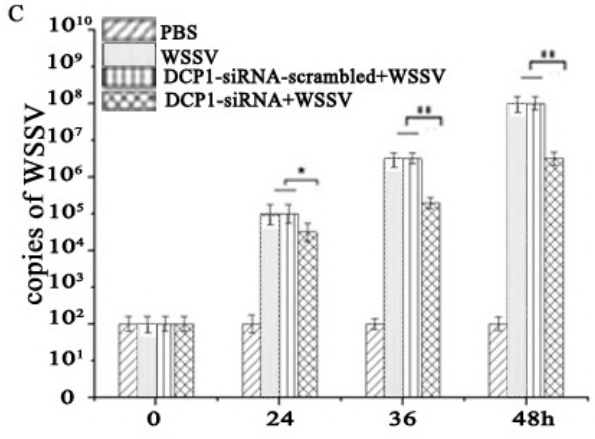
C
PBS
WSSV
DCP1-siRNA-scrambled+WSSV
DCP1-siRNA+WSSV
copies of WSSV
10¹⁰
10⁹
10⁸
10⁷
10⁶
10⁵
10⁴
10³
10²
10¹
0
*
**
**
0
24
36
48h

Fig 4

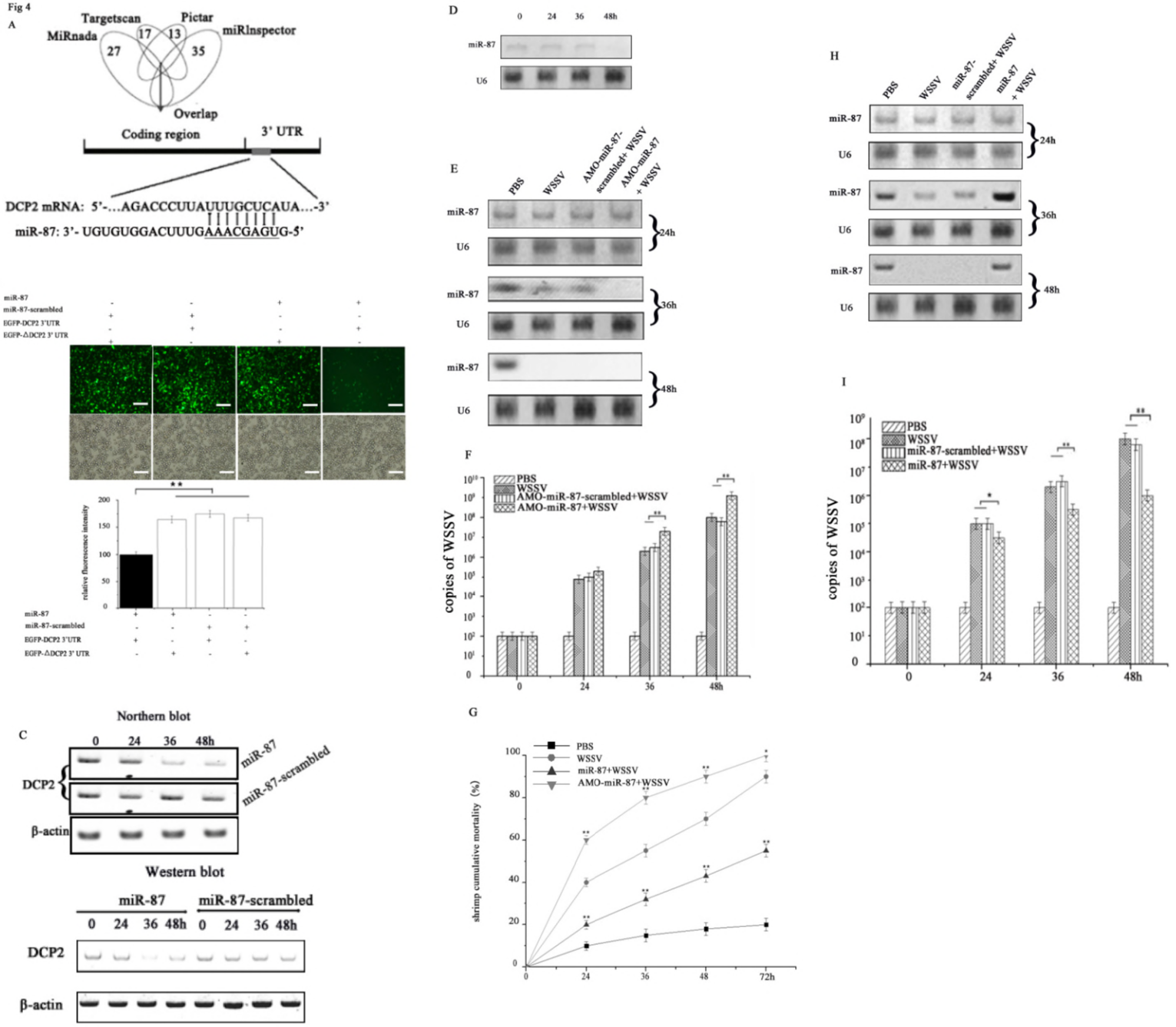
A
Targetscan
Pictar
MiRnada
miRInspector
17
13
27
35
Overlap
Coding region
3' UTR
DCP2 mRNA: 5'-…AGACCCUUAUUUGCUCAUA…-3'
miR-87: 3'- UGUGUGGACUUUGAAACGAGUG-5'
B
miR-87
miR-87-scrambled
EGFP-DCP2 3'UTR
EGFP-ΔDCP2 3' UTR
relative fluorescence intensity
C
Northern blot
0 24 36 48h
miR-87
miR-87-scrambled
DCP2
β-actin
Western blot
miR-87
miR-87-scrambled
0 24 36 48h 0 24 36 48h
DCP2
β-actin
D
0 24 36 48h
miR-87
U6
E
PBS
WSSV
AMO-miR-87-scrambled+ WSSV
AMO-miR-87 + WSSV
miR-87
U6
24h
36h
48h
F
PBS
WSSV
AMO-miR-87-scrambled+WSSV
AMO-miR-87+WSSV
copies of WSSV
G
PBS
WSSV
miR-87+WSSV
AMO-miR-87+WSSV
shrimp cumulative mortality (%)
H
PBS
WSSV
miR-87-scrambled+ WSSV
miR-87 + WSSV
miR-87
U6
24h
36h
48h
I
PBS
WSSV
miR-87-scrambled+WSSV
miR-87+WSSV
copies of WSSV

Fig 5

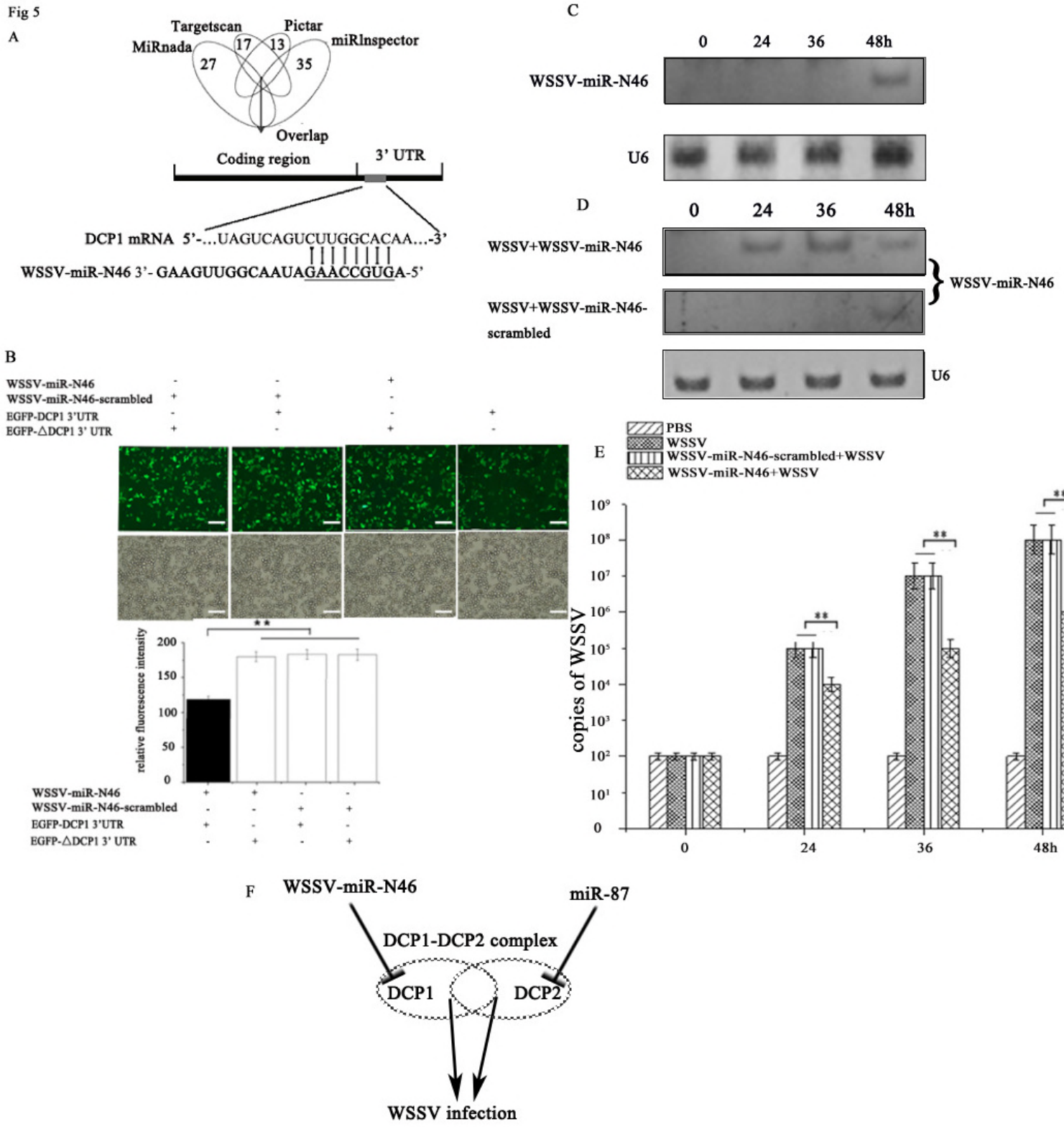
A
Targetscan
Pictar
MiRnada
miRInspector
17
13
27
35
Overlap
Coding region
3' UTR
DCP1 mRNA 5'-...UAGUCAGUCUUGGCACAA...-3'
WSSV-miR-N46 3'- GAAGUUGGCAAUAGAACCGUGA-5'
C
0
24
36
48h
WSSV-miR-N46
U6
D
WSSV+WSSV-miR-N46
WSSV-miR-N46
WSSV+WSSV-miR-N46-scrambled
U6
B
WSSV-miR-N46
WSSV-miR-N46-scrambled
EGFP-DCP1 3'UTR
EGFP-ΔDCP1 3' UTR
relative fluorescence intensity
E
PBS
WSSV
WSSV-miR-N46-scrambled+WSSV
WSSV-miR-N46+WSSV
copies of WSSV
F
WSSV-miR-N46
miR-87
DCP1-DCP2 complex
DCP1
DCP2
WSSV infection